

# Maps of the Little Bangs Through Energy Density and Temperature Fluctuations

Sumit Basu<sup>1</sup>\*, Rupa Chatterjee\*, Basanta K. Nandi<sup>†</sup> and Tapan K. Nayak\*

\*Variable Energy Cyclotron Centre, 1/AF Bidhan Nagar, Kolkata - 700064, India

<sup>†</sup>Indian Institute of Technology Bombay, Mumbai - 400076, India

**Abstract.** Heavy-ion collisions at ultra-relativistic energies are often referred to as little bangs. We propose for the first time to map the heavy-ion collisions at ultra-relativistic energies, similar to the maps of the cosmic microwave background radiation, using fluctuations of energy density and temperature in small phase space bins. We study the evolution of fluctuations at each stage of the collision using an event-by-event hydrodynamic framework. We demonstrate the feasibility of making fluctuation maps from experimental data and its usefulness in extracting considerable information regarding the early stages of the collision and its evolution.

**Keywords:** Big Bang, Quark-Gluon Plasma, CMBR, event-by-event hydro, correlations, fluctuations, Temperature, Little Bang, spectra

**PACS:** 25.75.-q, 25.75.Nq, 12.38.Mh

Observation of the cosmic microwave background radiation (CMBR) by various satellites confirms the Big Bang evolution, inflation and provide important information regarding the early Universe and its evolution with excellent accuracy [1, 2, 3]. The physics of heavy-ion collisions at ultra-relativistic energies, popularly known as little bangs, has often been compared to the Big Bang phenomenon of early Universe [4, 5, 6, 7, 8]. The matter produced at extreme conditions of energy density ( $\epsilon$ ) and temperature ( $T$ ) in heavy-ion collisions is a Big Bang replica in a tiny scale. In little bangs, the produced fireball goes through a rapid evolution from an early state of partonic quark-gluon plasma (QGP) to a hadronic phase, and finally freezes out within a few tens of fm. Heavy-ion experiments are predominantly sensitive to the conditions that prevail at the later stage of the collision as majority of the particles are emitted near the freeze-out. As a result, a direct and quantitative estimation of the properties of hot and dense matter in the early stages and during each stage of the evolution has not yet been possible.

In this manuscript, we propose to make temperature fluctuation maps, and use fluctuation measures to quantitatively probe the early stages of the heavy-ion collisions. We demonstrate the making of fluctuation maps in bins of rapidity ( $y$ ) and azimuthal angle ( $\phi$ ) from the AMPT event generator [9], which is a proxy for experimental data. These maps can be used to make a detailed analysis similar to those of the CMBR fluctuation methods [5, 8, 7, 6]. We use hydrodynamics to model the evolution of the produced system and make maps of  $\epsilon$  and  $T$  from initial time to freeze-out, and to estimate their relative fluctuations. By making a correspondence of measured fluctuations with

---

<sup>1</sup> corresponding author : sumit.basu@cern.ch

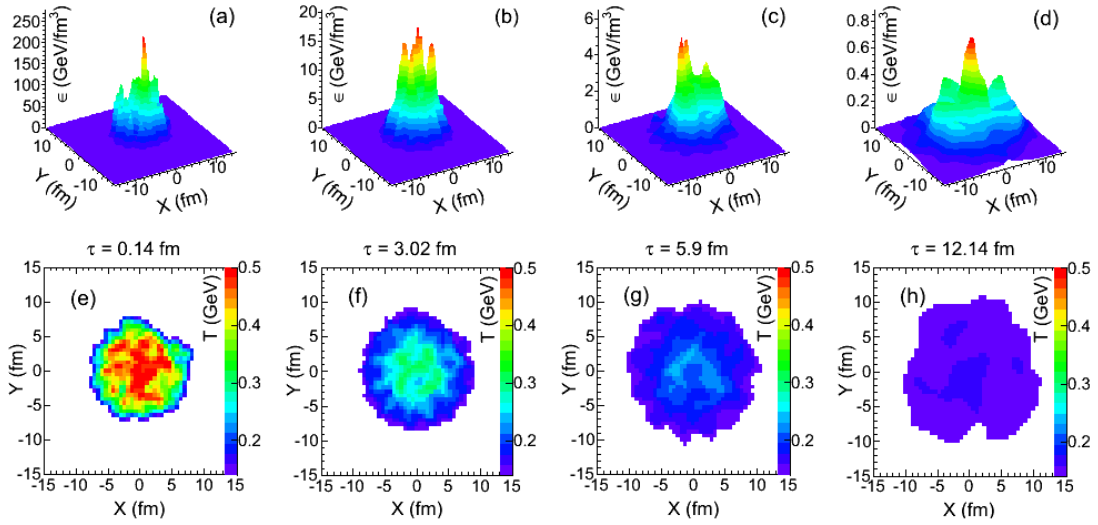


**FIGURE 1.** (Color online). Distributions of energy density (upper panels) and temperature (lower panels) in the transverse ( $X$ - $Y$ ) plane at four proper times ( $\tau$ ), obtained from hydrodynamic calculations for one central Pb-Pb event at  $\sqrt{s_{NN}} = 2.76$  TeV.

the time evolution profiles of the fluctuations from hydrodynamic calculations, we show that it is possible to visualize the thermodynamic conditions of colliding matter that presumably existed at different stages of evolution. Furthermore, we take advantage of the large number of particles produced in the heavy-ion collisions to obtain transverse momentum ( $p_T$ ) distribution and extract the temperature from each event. We demonstrate that event-by-event temperature fluctuations can be used to provide important thermodynamic parameters for the system created in the collisions [10, 11, 12, 13, 14, 15, 16].

Recent experimental data from the Relativistic Heavy Ion Collider (RHIC) and the Large Hadron Collider (LHC) have confirmed the formation of a strongly coupled system. Hydrodynamics has been used extensively and to a large extent successfully to explain majority of these experimental results [17]. A (2+1)-dimensional event-by-event ideal hydrodynamical framework [18] is used in the present work to model the space-time evolution of the system produced in most central (0–5% of the total cross section) collisions of lead nuclei at  $\sqrt{s_{NN}} = 2.76$  TeV at LHC. A lattice-based equation of state [19] is used in this model and 170 MeV is considered as the transition temperature from the QGP to a hadronic phase. This model has been successfully used to explain the spectra and elliptic flow of hadrons at RHIC and LHC energies [18]. In this Monte Carlo Glauber model, the standard two-parameter Woods-Saxon nuclear density profile is used to distribute the nucleons randomly into the colliding nucleons. Two nucleons from different nuclei are assumed to collide when  $d^2 < \sigma_{NN}/\pi$ , where  $d$  is the transverse distance between the nuclei and  $\sigma_{NN}$  is the inelastic nucleon-nucleon cross section. For LHC energies, we take  $\sigma_{NN} = 64$  mb and the initial formation time of the plasma  $\tau_0 = 0.14$  fm [21, 18, 20]. A wounded nucleon (WN) profile is considered where the initial entropy density is distributed around the WN using a 2-dimensional Gaussian

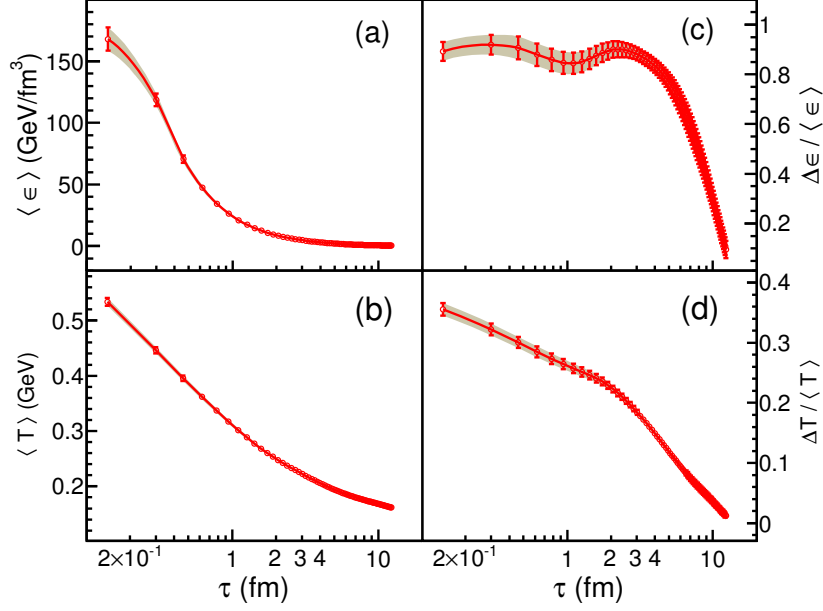


**FIGURE 2.** (Color online). Temporal evolution of (a) average energy density, (b) average temperature, (c) fluctuations in energy density, and (d) fluctuations in temperature, for central Pb-Pb collisions at  $\sqrt{s_{\text{NN}}} = 2.76$  TeV, obtained from hydrodynamic calculations. The shaded regions represent the extent of event-by-event variations.

distribution function,

$$s(X, Y) = \frac{K}{2\pi\sigma^2} \sum_{i=1}^{N_{\text{WN}}} \exp\left(-\frac{(X - X_i)^2 + (Y - Y_i)^2}{2\sigma^2}\right). \quad (1)$$

Here  $X_i, Y_i$  are the transverse coordinates of the  $i^{\text{th}}$  nucleon and  $K$  is an overall normalization constant. The size of the density fluctuations is determined by the free parameter  $\sigma$ , which is taken to be 0.4 fm [18]. The temperature at freeze-out is taken as 160 MeV, which reproduces the measured  $p_{\text{T}}$  spectra of charged pions at LHC.

Figure 1 shows the distributions of  $\epsilon$  and  $T$  for a single event in  $X$ - $Y$  bins (each bin is of size 0.6 fm  $\times$  0.6 fm) at four different values of proper time ( $\tau$ ). The upper panels (a-d) show a three dimensional view of  $\epsilon$ , whereas the lower panels (e-h) show the  $T$  variations in the transverse plane. At early times, sharp and pronounced peaks in  $\epsilon$  and hotspots in  $T$  are observed. These bin-to-bin fluctuations in  $\epsilon$  and  $T$  indicate that the system formed immediately after collision is inhomogeneous in phase space and quite violent. As time elapses, the system cools, expands, and the bin-to-bin variations in  $\epsilon$  and  $T$  smoothens out tending towards a homogenous system at freeze-out.

Observations from Fig. 1 can be quantified by studying the mean energy density ( $\langle \epsilon \rangle$ ), mean temperature ( $\langle T \rangle$ ) over all the bins, and the bin-to-bin fluctuations of  $\epsilon$  and  $T$  at each  $\tau$ . Figure 2 presents the time evolution of  $\langle \epsilon \rangle$  and  $\langle T \rangle$ , and their fluctuations. The  $x$ -axes are plotted in logarithmic scale for zooming in on the early times. The event-by-event variations of these quantities are represented by the shaded regions, taken from

about 500 events. The  $\langle \varepsilon \rangle$  and  $\langle T \rangle$  decrease as time elapses. The value of  $\langle \varepsilon \rangle$  falls sharply from  $\sim 168 \text{ GeV/fm}^3$  at  $\tau = 0.14 \text{ fm}$  to a value of  $\sim 20 \text{ GeV/fm}^3$  at  $\tau = 1 \text{ fm}$ , and then falls slowly till freeze-out. The initial energy density values are close to the results from the ALICE collaboration,  $\varepsilon \tau \sim 16 \text{ GeV/fm}^2$  [22]. On the other hand, the fall of  $\langle T \rangle$  with  $\tau$  is smooth, which goes down from  $\sim 530 \text{ MeV}$  at  $\tau = 0.14 \text{ fm}$  to  $\sim 300 \text{ MeV}$  at  $\tau = 1 \text{ fm}$ . At the freeze-out,  $\langle T \rangle$  is close to  $160 \text{ MeV}$ .

The bin-to-bin fluctuations in  $\varepsilon$  and  $T$  have been quantified by  $\Delta\varepsilon/\langle\varepsilon\rangle$  and  $\Delta T/\langle T\rangle$ , where  $\Delta\varepsilon$  and  $\Delta T$  are the root mean square (RMS) deviations. Time evolutions of fluctuations in  $\varepsilon$  and  $T$  are presented in the right panels of Fig. 2. Extremely large fluctuations in energy density of  $\sim 90\%$  are observed at early times, confirming the violent nature of the collision. At the same time, the fluctuations in  $T$  are smaller ( $\sim 35\%$ ). Interestingly, although  $\langle\varepsilon\rangle$  decreases quite fast, the fluctuation in  $\varepsilon$  remains almost constant up to  $\tau \sim 2.5 \text{ fm}$ , then falls rapidly. Around the same value of  $\tau$ , the fluctuation in  $T$  shows a kink, where the change in fluctuation increases. There may be a characteristic change in the behavior of the system at this  $\tau$  during the hydrodynamic evolution. A close analysis of the time evolution of different phases indicates that these changes in nature of the fluctuations happen at a time when the hadronic phase starts to dominate over the QGP phase.

Fluctuation measurements in heavy-ion experiments are possible only at freeze-out. The connection from the freeze-out to the early stages of collision can be made by comparing experimental data with theoretical calculations at freeze-out. A large number of particles produced in every central Pb-Pb collision at  $\sqrt{s_{\text{NN}}} = 2.76 \text{ TeV}$  makes it possible to construct  $m_T$  spectrum of identified particles in every event. Fitting the  $m_T$  distribution of pions with a Maxwell-Boltzmann distribution yields the value of the effective temperature,  $T_{\text{evt}}$ , in each event. This temperature is related to the  $\langle m_T \rangle$  of pions within the same acceptance:

$$\langle m_T \rangle = \frac{2T^2 + 2m_0T + m_0^2}{m_0 + T}, \quad (2)$$

where  $m_0$  is the mass of pion and  $T$  is the temperature. From the generated events, it is verified that for pions within the central rapidity ( $-0.5 < y < 0.5$ ) and full azimuth and  $m_0 \leq m_T \leq 1.5 \text{ GeV}$ , the value of  $T_{\text{evt}}$  from fitting the  $m_T$  spectrum as well as from  $\langle m_T \rangle$  are close to each other. The upper limit of  $m_T$  is chosen to exclude pions affected by jets. Figure 3 shows the distributions of  $\langle m_T \rangle$  of pions and corresponding values of  $T_{\text{evt}}$  calculated using the above expression for a large number of events. It should be noted that the values of  $T_{\text{evt}}$  have contributions from both a thermal part and a second component which depends on the collective transverse velocity ( $\langle \beta_T \rangle$ ) of the system. For a narrow centrality event class, assuming the transverse velocity to be same for all events, the fluctuation in  $T_{\text{evt}}$  may be a good representation of the temperature fluctuation.

Fluctuation in event-by-event temperature has been expressed in terms of  $\Delta T_{\text{evt}}/\langle T_{\text{evt}} \rangle$ , called the global fluctuation. This fluctuation has contributions from both the statistical and dynamical components. Statistical component has been estimated by constructing synthetic events, whose  $\langle m_T \rangle$  and  $T_{\text{evt}}$  distributions are also shown in Fig. 3. The dynamical component of the global temperature fluctuation has been calculated to be  $1.8\%$ . This value corresponds to heat capacity of  $C_V = 3067$ . This is the first estimation of heat capacity at LHC energies from model calculations.

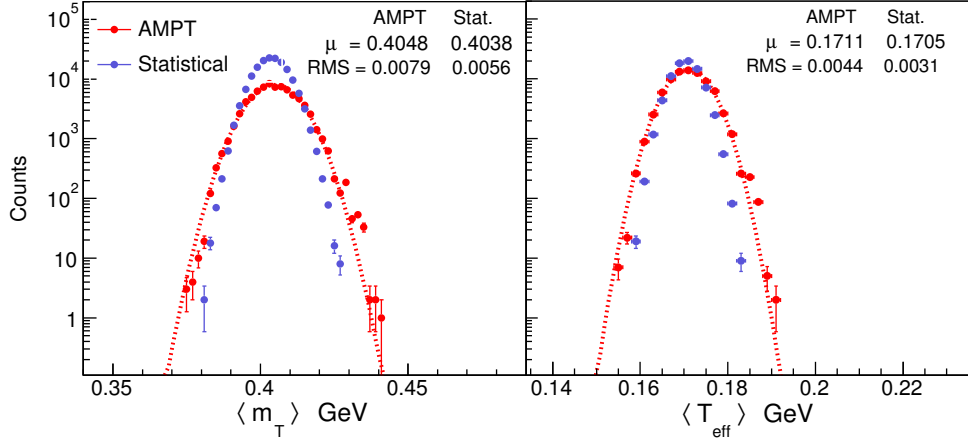


**FIGURE 3.** (Color online). Event-by-event distribution of  $\langle m_T \rangle$  and corresponding  $T_{\text{evt}}$  for pions within one unit of rapidity and full azimuth for central Pb-Pb collisions at  $\sqrt{s_{\text{NN}}} = 2.76$  TeV using AMPT.

Local temperature fluctuations provide the amount of non-uniformity within a single event. This is studied by dividing the available phase space to several  $y$ - $\phi$  bins, and estimating the bin temperature ( $T_{\text{bin}}$ ) as per Eq.(3). For a given event, local temperature fluctuations in the  $y$ - $\phi$  bins has been expressed as:

$$F_{\text{bin}} = (T_{\text{bin}} - T_{\text{evt}})/T_{\text{evt}}. \quad (3)$$

For each event, the values of  $F_{\text{bin}}$  in the  $y$ - $\phi$  bins provide a fluctuation map. We choose events with 0–5% centrality window to ensure that the event-to-event variation in the number of participating nucleons is minimal.

The phase space around the central rapidity ( $-0.5 \leq y \leq 0.5$ ) and full azimuth ( $-\pi \leq \phi \leq \pi$ ) is divided into a number of bins in  $y$ - $\phi$ . We present results of the calculation with a grid of  $6 \times 6$  bins, where the bin sizes are well within the detector resolutions for the present experiments at RHIC and LHC. For a typical event, the temperature fluctuation map for  $6 \times 6$  bins in central rapidity and full azimuth is shown in Fig. 4. The map gives a quantitative view of the temperature fluctuation in the available phase space for an event where the fluctuation is represented by different color pallets. The map shows several hot (red) as well as cold (blue) zones, and zones with average (green) fluctuation throughout the phase space. The hot and cold zones may have their origin from the extreme regions of phase space that existed during the early stages of the reaction.

The amount of local temperature fluctuation for a single event is quantified by the ratio of RMS to the mean of the  $T_{\text{bin}}$  distribution. The event-by-event distribution of the local fluctuation is shown in Fig. 6 for  $\langle m_T \rangle$  (left panel) and temperature (right panel). Statistical component of the local fluctuations has been extracted from synthetic events, which is also shown in Fig. 6. The average dynamical local fluctuation, extracted after subtracting the statistical component, has been estimated to be 7.2%. The non-zero value of local fluctuation may imply that these might have the contributions from the early state fluctuations.

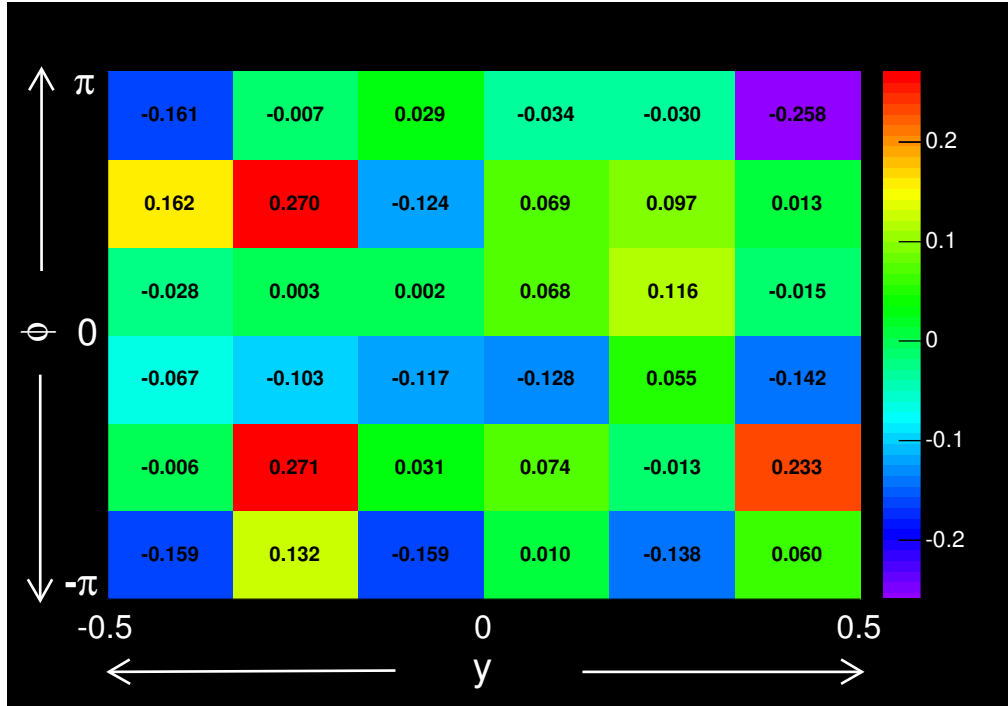


**FIGURE 4.** (Color online). Temperature fluctuation map in  $y$ - $\phi$  bins for central Pb-Pb collisions at  $\sqrt{s_{\text{NN}}} = 2.76$  TeV using the AMPT model. For each  $y$ - $\phi$  bin, fluctuation is expressed as  $(T_{\text{bin}} - T_{\text{evt}})/T_{\text{evt}}$ , the deviation of the bin temperature to the event temperature. The color palettes indicate the magnitude of fluctuations.

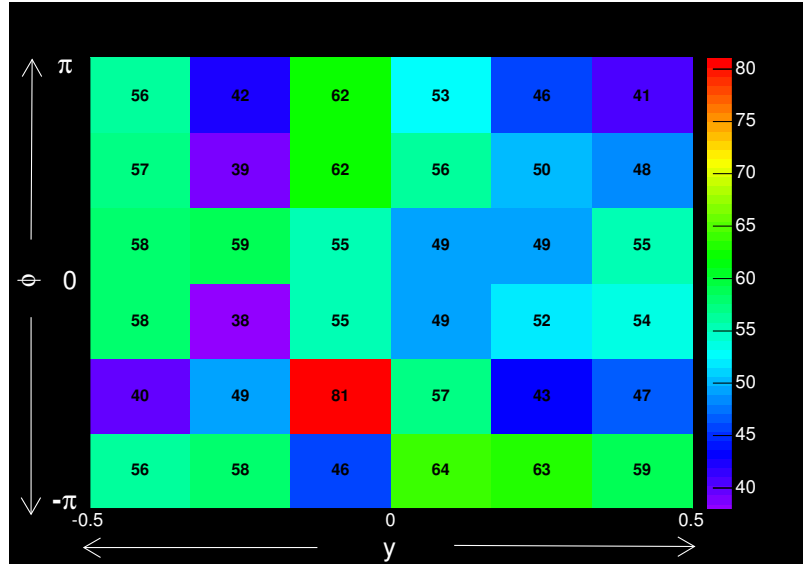


**FIGURE 5.** (Color online). Event-by-event local pion number fluctuations, obtained from  $6 \times 6$   $y$ - $\phi$  bins in central rapidity and full azimuth for central Pb-Pb collisions at  $\sqrt{s_{\text{NN}}} = 2.76$  TeV using the AMPT event generator.

There was strong assumptions and predictions that the local temperature fluctuations has a strong correlations between charge fluctuations and charge particle number. In the AMPT model that pion number distributions (fluctuations) in local phase space has no correlations with the temperature fluctuations in that given phase space for that particular event is shown in Fig. 5. Fig. 4 and Fig. 5 are given one another to have the idea for a particular event how it looks like for the model. It would be very interesting to see same plot in data points how it shapes. These pion number fluctuations in event by event basis and within a event local distributions are related to to isothermal compressibility.

In cosmic microwave background radiation (CMBR) studies, the temperature fluctuation map confirms the Big Bang evolution, inflation and provides information regarding the early Universe. The temperature fluctuation map of every event is similar to the fluctuation map of the CMBR.

The map gives a quantitative view of the temperature fluctuations in the available phase space. It clearly shows several hot (red) as well as cold (blue) spots, with average (green) zones throughout the phase space. These spots may have their origin from the extreme regions of phase space, which existed during the early stages of the reaction. This may indicate that the observed fluctuations are remnants of the initial energy density fluctuations and are not washed out until the freeze-out stage. The amount of these fluctuations are similar to those from hydrodynamic calculations at  $\tau \sim 12$  fm. Thus, within the present theoretical framework, we can make a correspondence to the early stage of the collision through the hydro calculations. Furthermore, these fluctuation maps can form the basis of power spectrum analysis [8, 7, 6].

In CMBR studies of the Big Bang, there is only one event, whereas in the case of heavy-ion collision experiments, one has access to very large number of events. This can be used as an advantage in order to gain access to the primordial state.

The present study may be affected by various effects, contributing to the global and local temperature fluctuations. Some of these are listed below: We discuss the following effects which can affect temperature fluctuations:

*Slopes from exponential distributions:* Similar fluctuation maps may be constructed from fluctuation of slopes of  $\langle m_T \rangle$  distribution by fitting. But it involves fitting error and due to limited no of particles slopes may not be accurate via fitting. A general methodology is followed via  $\langle m_T \rangle$  of pions instead of transverse momentum ( $\langle p_T \rangle$ ) of charged particle spectra [28]. However,  $\langle p_T \rangle$  may not be a good measure of the temperature [12].

*Event plane orientation:* Event plane orientation is necessary for studying bin-to-bin fluctuations, especially for non-central collisions. For the present study, AMPT events are event plane oriented.

*Effect of radial flow and azimuthal anisotropy:* Fourier decomposition of the momentum distribution in transverse plane yields a  $\phi$ -independent, axially symmetric radial flow component and a  $\phi$ -dependent part containing the anisotropic flow coefficients. For most central collisions within a narrow centrality bin, radial flow remains similar for all the events and the anisotropic flow components do not affect the slope of the  $m_T$  distribution.

*Final state effects:* Final state effects, such as resonance decay, and hadronic rescattering tend to make the  $m_T$  spectra softer. The choice of the  $m_T$  window has to be made in order to minimize such effects.

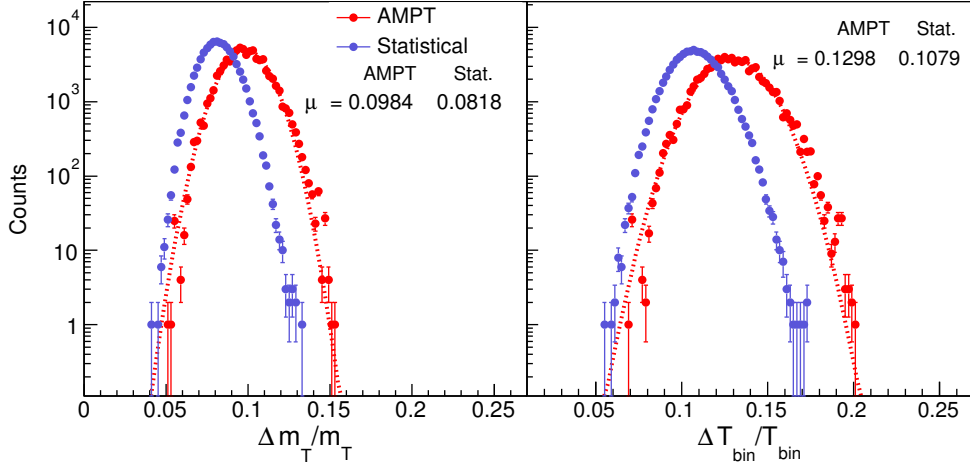


**FIGURE 6.** (Color online). Event-by-event local temperature fluctuations, obtained from  $6 \times 6$   $y$ - $\phi$  bins in central rapidity and full azimuth for central Pb-Pb collisions at  $\sqrt{s_{NN}} = 2.76$  TeV using the AMPT event generator.

*Finite multiplicity effect and the number of  $y$ - $\phi$  bins:* The number of  $y$ - $\phi$  bins has been chosen by taking into account finite number of particles in each bin so that multiplicity fluctuations do not affect the estimation of  $m_T$ . The amount of local fluctuation will have variation with the number of  $y$ - $\phi$  bins. Pb-Pb collisions at LHC energies produce a large number of particles which are adequate for event-by-event studies. The number bins in constructing the map should not be too large in order to avoid the empty bin effect.

*Event averaging:* Temperature fluctuation map involves constructing the  $m_T$  spectrum in a given  $y$ - $\phi$  bin by including particles from a large number of events. As the final spectrum is event averaged, the averaging does not affect the determination of slope parameters.

*Species dependence:* As the particle production mechanism of baryons, mesons and strange particles are different, species dependence of temperature fluctuations may provide extra information of their freeze-out hyper-surfaces. Whether the origin of the temperature fluctuations are solely due to initial state fluctuations or any final state effect, this will be interesting to study in the species dependence of temperature fluctuations.

*Viscosity effect:* Viscosity tends to dilute the fluctuations. The SM version of AMPT includes the effect of viscosity ( $\eta/s \sim 0.15$  at  $T=436$  MeV [23, 26]). Analysis using a viscous hydrodynamic model is in progress.

In conclusion, we have shown that temperature fluctuation maps, similar to those in CMBR experiments, offer a novel way of representing data in heavy-ion collisions. Experimentally, it is possible to obtain bin-to-bin fluctuations in temperature from the transverse momentum distributions in  $y$ - $\phi$  bins. Interestingly, quantitative similar fluctuations are obtained from hydrodynamic model calculations for most central Pb-Pb collisions at the LHC. Non-zero fluctuations imply that some of the signals of the initial state fluctuations remain as imprints at the freeze-out, this connection has been estab-



lished within the framework of a hydrodynamic model. Important information like the speed of sound, specific heat, etc., can be extracted from event-by-event temperature fluctuations. Relativistic hydrodynamic calculations have been used to understand the evolution of  $\varepsilon$  and  $T$  temperature fluctuations. It shows that the system exhibits fiercely large fluctuations at early times, which diminish with the elapse of time.

The feasibility of studying temperature fluctuations in Pb-Pb collisions at  $\sqrt{s_{NN}}=2.76$  TeV has been demonstrated by using simulated events from the AMPT model. Temperatures are extracted from  $\langle m_T \rangle$  of charged pions. The global fluctuation in the event temperature has been extracted to be 1.8%. The value of heat capacity has been calculated as  $C_V = 3067$ . At the LHC, the phase transition is predicted to be a cross over. Thus the transition may not take place at a unique point in the phase diagram, which contributes to the entropy and temperature fluctuations. The estimation of the heat capacity helps in understanding of the nature of the phase transition. At the same time, the variation of  $C_V$  as a function of beam energy at RHIC can be used to probe the QCD critical point. Local temperature fluctuations over small phase bins within each event have been extracted to be 7.2% for  $6 \times 6$  bins in central rapidity. Although the initial fluctuations are expected to be diluted until the freeze-out, the observation of local fluctuations imply that some amount of fluctuation may survive, affecting the particle spectra and flow. The present study in conjunction with theoretical model calculations open up new avenues for characterizing the heavy-ion collisions, and are useful in obtaining proper insight into the evolution of the collision.

We emphasize that this novel way of studying temperature fluctuations will open new avenues of studying heavy-ion collisions and will be useful in obtaining proper insight into the little bang and QGP matter.

We would like to thank H. Holopainen for providing us with the event-by-event hydrodynamic code. We gratefully acknowledge stimulating discussions with Steffen Bass, Satyajit Jena, Krishna Rajagopal, Dinesh Srivastava, Bikash Sinha, Roberto Preghenella, Alexander Philipp Kalweit, Jurgen Schukraft, Zi-Wei Lin.

## REFERENCES

1. E. Komatsu and C. L. Bennett (WMAP science team) arXiv:1404.5415 [astro-ph.CO].
2. A.I. Fisenko and V. Lemberg, arXiv:1401.1432 [astro-ph.CO].
3. P.A.R. Ade *et al.* (Planck Collaboration), arXiv:1303.5062 [astro-ph.CO].
4. W. Florkowski, Phenomenology of Ultra-relativistic Heavy-ion Collisions, World Scientific, 2010.
5. U. Heinz, J. Phys.: Conf. Ser. **455**, 012044 (2013).
6. P. Naselsky *et al.* Phys. Rev. **C 86**, 024916 (2012).
7. A. Mocsy and P. Sorensen, Nucl. Phys. **A 855**, 241 (2011).
8. A.P. Mishra *et al.*, Phys. Rev. **C 77**, 064902 (2008); *ibid.*, Phys. Rev. **C 81**, 034903 (2010).
9. Z.-W. Lin, C.M. Ko, B.-A. Li, B. Zhang, S. Pal, Phys. Rev. **C 72**, 064901 (2005).
10. L. Stodolsky, Phys. Rev. Lett. **75**, 1044 (1995).
11. R. Korus *et al.*, Phys. Rev. **C 64**, 054908 (2001).
12. M.A. Stephanov, K. Rajagopal and E. V. Shuryak, Phys. Rev. **D 60**, 114028 (1999).
13. R. Gavai, S. Gupta and S. Mukherjee, Phys. Rev. **D 71**, 074013 (2005).
14. G. Wilk and Z. Wlodarczyk, Phys. Rev. Lett. **84**, 2770 (2000).
15. E.V. Shuryak, Phys. Lett. **B 423**, 9 (1998).
16. S. Mrowczynski, Phys. Lett. **B 430**, 9 (1998).

17. H. Song, arXiv:1401.0079v1 [nucl-th].
18. H. Holopainen, H. Niemi, and K. Eskola, Phys. Rev. **C 83**, 034901 (2011).
19. M. Laine and Y. Schroder, Phys. Rev. **D 73**, 085009 (2006).
20. R. Chatterjee, H. Holopainen, T. Renk, and K. J. Eskola, Phys. Rev. **C 83**, 054908 (2011).
21. R. Paatelainen, K.J. Eskola, H. Holopainen, and K. Tuominen, Phys. Rev. **C 87**, 044904 (2013).
22. K. Aamodt *et al.*, (ALICE Collaboration), Phys. Rev. Lett. **105**, 252301 (2010); A. Toia (ALICE Collaboration), Jour. Phys. **G 38**, 124007 (2011).
23. S. Pal and M. Bleicher, Phys. Lett. **B 709**, 82 (2012).
24. J. Xu and C.M. Ko, Phys. Rev. **C 83**, 034904 (2011).
25. J. Xu and C.M. Ko, Phys. Rev. **C 84**, 014903 (2011).
26. D. Solanki, P. Sorensen, S. Basu, R. Raniwala, T.K. Nayak, Phys. Lett. **B 720**, 352 (2013).
27. B. Abelev *et al.* (ALICE Collaboration), Phys. Rev. Lett. **109**, 252301 (2012).
28. H. Appelshauser *et al.* (NA49 Collaboration), Phys. Lett. **B 459**, 679 (1999).